CHEMPLUSCHEM

DOI: 10.1002/cplu.201200006

Dual Emitting [Yb(5,7ClQ)$_2$(H5,7ClQ)$_2$Cl]: Chemical and Photophysical Properties**

Flavia Artizzu,*[a] Francesco Quochi,[b] Michele Saba,[b] Luciano Marchiò,[c] Davide Espa,[a] Angela Serpe,[a] Andrea Mura,[b] Maria Laura Mercuri,[a] Giovanni Bongiovanni,[b] and Paola Deplano*[a]

The anhydrous hepta-coordinated [Yb(5,7ClQ)$_2$(H5,7ClQ)$_2$Cl] complex bearing two quinolinolato ligands in the lanthanide coordination sphere and two quinolinol ligands in the zwitterionic form as well as one chloride atom, has been synthesized and fully characterized. This compound exhibits dual luminescence in the near infrared (NIR; metal-centered) and in the visible (ligand-centered) spectral regions. Ligand emission is strongly influenced by π–π interactions in the crystal packing. Photophysical studies were applied to evaluate the quenching processes affecting the Yb^{3+} NIR luminescence as well as to highlight the ligand-to-metal sensitization mechanism. The ligand-to-metal sensitization efficiency parameter was determined to be close to unity, thus showing that the quinolinolato ligand acts as a very efficient antenna funneling energy absorbed from UV and visible light toward Yb^{3+}. Time-resolved photoluminescence studies and transient absorption experiments clearly demonstrate that the ligand-to-metal energy-transfer process occurs on an ultrafast timescale and involves the triplet states of the ligand. Very similar Yb^{3+} emission lifetimes near 1 μm are observed for a solution in DMSO (7.85 μs) and for solid-state crystals (7.10 μs). The unusually short radiative lifetime of 690 μs, which was determined from spectroscopic data from a solution in DMSO, shows that the Yb ion in this complex has a remarkably high radiative strength. A low quantum yield of the NIR luminescence, $\Phi_{tot} = 1.4 \times 10^{-2}$, was found. The deactivation rate of lanthanide ions through vibrational excitation of CH groups was assessed in the framework of the Förster theory of resonance energy transfer. According to this model, energy transfer to CH groups only partially explains the observed NIR luminescence quenching.

Introduction

Near-Infrared (NIR) emitting lanthanide (Er^{3+}, Nd^{3+}, Yb^{3+}) quinolinolate complexes are currently receiving widespread attention as low-cost functional materials for possible applications in several fields spanning from optoelectronics to biology/biomedicine.[1–9] The quinolinolato ligands are conveniently employed as light-harvesting "antennas" for resonance energy transfer (RET) to the higher energy levels of the lanthanide ion (sensitized emission),[10–17] to overcome the very small absorption coefficients of the lanthanide-based line-like absorption transitions, which are related to parity-forbidden intrashell transitions between 4f orbitals. Through this indirect sensitization process, NIR radiation can in fact be obtained upon photoexcitation of the antenna with a low-cost, near UV/visible source. For this reason, such compounds can be seen as light conversion molecular devices (LCMDs).[18]

Despite the recent interest in these compounds, there is a lack in optimized synthetic procedures for their preparation and the structures of lanthanide quinolinolates are not available. This has led in some instances to questionable assignments of the deactivation mechanisms affecting the luminescence properties. This prompted us and other research groups to combine chemical and photophysical studies on well characterized samples to achieve a reliable structure–property relationship,[19–22] and to provide a description of the role of the most important quenchers such as CH groups and water that are in close proximity of the metal center in the nonradiative decay processes which affect the quantum yield of erbium quinolinolates.[23] Moreover, photophysical studies have shown that in these complexes ligand-to-metal energy transfer is exceptionally efficient leading to erbium sensitization efficiency up to the population inversion threshold, as confirmed by the results of time-resolved studies on the intraligand and ligand-to-metal excited-state temporal dynamics, which also indicate that this mechanism is a two-step process involving the triplet level of the quinolinolato ligand.[11,24]

In this study, we have investigated ytterbium quinolinolates and report herein chemical and photophysical studies on the

[a] Dr. F. Artizzu, Dr. D. Espa, Dr. A. Serpe, Prof. M. L. Mercuri, Prof. P. Deplano
Dipartimento di Chimica Inorganica e Analitica, University of Cagliari
SS 554 Bivio per Sestu, I-09042, Monserrato-Cagliari (Italy)
Fax: (+39) 0706754456
f.artizzu@unica.it
deplano@unica.it

[b] Dr. F. Quochi, Dr. M. Saba, A. Mura, Prof. G. Bongiovanni
Dipartimento di Fisica, University of Cagliari
SS 554 Bivio per Sestu, I-09042, Monserrato-Cagliari (Italy)

[c] Dr. L. Marchiò
Dipartimento di Chimica Generale e Inorganica
Chimica Analitica, Chimica Fisica, University of Parma
Parco Area delle Scienze 17A, I-43100 Parma (Italy)

[**] H5,7ClQ = 5,7-dichloro-8-quinolinol.

Supporting information for this article is available on the WWW under http://dx.doi.org/10.1002/cplu.201200006.

neutral anhydrous ytterbium tetrakis-type complex: [Yb(5,7ClQ)$_2$(H5,7ClQ)$_2$Cl], (H5,7ClQ = 5,7-dichloro-8-quinolinol), where the Yb^{3+} is coordinated to two anionic quinolinolato ligands and to two quinolinol ligands in the zwitterionic form, with a chloride ion completing the metal coordination sphere. In addition to studying the emission properties of this compound, our goal is to reach a full understanding of the ligand-to-metal sensitization mechanism which has not been clarified up to now. Moreover, quenching effects on the Yb^{3+} emission resulting from vibrational coupling with CH groups of the ligand were experimentally evaluated. To these purposes, ytterbium radiative lifetime and ligand-to-metal sensitization efficiency—data which are often neglected in the literature—were determined.

Results and Discussion

Synthesis and description of the crystal structure

The [Yb(5,7ClQ)$_2$(H5,7ClQ)$_2$Cl] complex (**YbClQ$_4$**) was prepared by treating 5,7-dichloro-8-quinolinol (H5,7ClQ) with $YbCl_3 \cdot 6H_2O$ in a solvent mixture of CH_3CN/CH_3OH (4:1). No addition of base was required to deprotonate the ligand because it exhibits increased acidity with respect to the unsubstituted 8-hydroxy-quinoline owing to the presence of electron-withdrawing halo groups.[25] The reaction mixture was then stirred under gentle heating (50–60 °C) for approximately one day and then the solution was carefully evaporated under reduced pressure until saturation (with the color of the solution turning to orange). Well-shaped red crystals suitable for X-ray structural analysis were obtained after slow evaporation of the solvent over a few days. A summary of the X-ray crystallographic data is reported in Table 1 and selected bond lengths are reported in Table 2. The Yb^{3+} ion is hepta-coordinated to four ligands, two of which are N,O-chelated mono-anions, and two others that can be formally considered as zwitterionic ligands (N^+–H and O^-) acting as monodentate oxygen donors. The charge of the metal ion is balanced by one coordinating chloride. Two independent molecules are present in the unit cell that are related by a (pseudo)center of symmetry, to form a dimeric arrangement of [{Yb(5,7ClQ)$_2$(H5,7ClQ)$_2$Cl}$_2$] (Figure 1). The coordination geometry of [Yb(5,7ClQ)$_2$(H5,7ClQ)$_2$Cl] can be described as distorted pentagonal bipyramid with the equatorial positions defined by Cl(1)-O(11)-O(13)-N(11)-N(13) for Yb(1), and Cl(2)-O(15)-O(17)-N(15)-N(17) for Yb(2). The two protonated quinoline units (II, IV) act as hydrogen-bond donors with the N^+–H moiety, which is directed toward the oxygen atoms of the opposite and N,O-chelated quinolines (I, III). Geometric parameters of the hydrogen bonds are reported in Table 3.

Table 1. Summary of X-ray crystallographic data for [{Yb(5,7ClQ)$_2$(H5,7ClQ)$_2$Cl}$_2$].

formula	$C_{72}H_{36}Cl_{18}Yb_2N_8O_8$	V [Å^3]	7297.7(11)
M_r	2125.27	Z	4
color, habit	orange, prism	T [K]	293
crystal size [mm]	0.45×0.30×0.22	ρ_{calcd} [Mg^{-3}]	1.934
crystal system	orthorhombic	μ [mm^{-1}]	3.271
space group	$Pca2_1$	θ range [°]	0.69 to 26.02
a [Å]	25.477(2)	reflns obs $F > 4\sigma(F)$	72355/14340
b [Å]	9.730(1)	GooF	0.616
c [Å]	29.439(2)	R_1[a]	0.0443
α [°]	90	wR_2[b]	0.0494
β [°]	90	–	–
γ [°]	90	–	–

[a] $R_1 = \Sigma||Fo|-|Fc||/\Sigma|Fo|$. [b] $wR_2 = [\Sigma[w(F_o^2-F_c^2)2]/\Sigma[w(F_o^2)2]]^1/_2$, $w = 1/[\sigma2(F_o^2) + (aP)2 + bP]$, where $P = [\max(F_o^2,0) + 2F_c^2]/3$.

Table 2. Selected bond lengths [Å] for [Yb(5,7ClQ)$_2$(H5,7ClQ)$_2$Cl]$_2$.

Bond	Bond length [Å]	Bond	Bond length [Å]
Yb(1)–O(11)	2.298(8)	Yb(2)–O(15)	2.293(8)
Yb(1)–O(12)	2.187(8)	Yb(2)–O(16)	2.185(9)
Yb(1)–O(13)	2.276(9)	Yb(2)–O(17)	2.248(8)
Yb(1)–O(14)	2.172(8)	Yb(2)–O(18)	2.158(8)
Yb(1)–N(11)	2.503(11)	Yb(2)–N(15)	2.479(11)
Yb(1)–N(13)	2.540(10)	Yb(2)–N(17)	2.528(10)
Yb(1)–Cl(1)	2.595(4)	Yb(2)–Cl(2)	2.597(4)

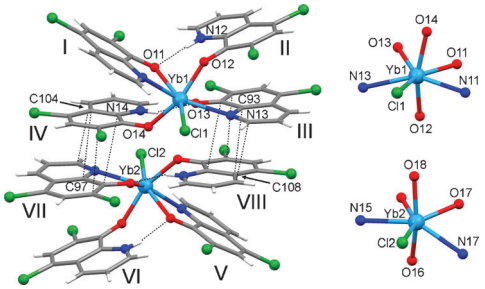

Figure 1. Left: Molecular structure of the [Yb(5,7ClQ)$_2$(H5,7ClQ)$_2$Cl]$_2$ moiety. Dashed bonds represent intermolecular π interactions and intramolecular hydrogen bonds. Right: Coordination environment of the Yb^{3+} ions.

Table 3. Geometric parameters of the hydrogen bonds of [Yb(5,7ClQ)$_2$(H5,7ClQ)$_2$Cl]$_2$.

Interaction	Bond distance [Å]	N–H···X [°]
N(12)···O(11)	2.75(1)	167.7(8)
N(14)···O(13)	2.96(2)	162.7(8)
N(16)···O(15)	2.75(2)	159.7(9)
N(18)···O(17)	2.87(1)	162.3(8)

The two independent molecules interact through a partial stack between the III–VIII and IV–VII quinoline molecules with the minimum distance between these stacks of 3.389(8) Å (C93···C108) and 3.463(8) Å (C97···C104), respectively. The crystal packing reveals the presence of layers that are approximately planar to the *ac* crystallographic plane. These layers are determined by the partial stack of the I–VI and II–V quinoline molecules (Figure 2).

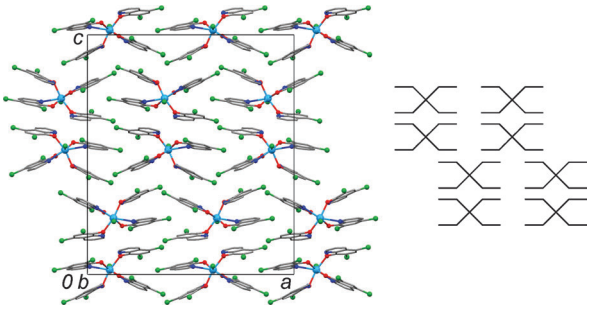

Figure 2. Crystal packing of **YbClQ$_4$** projected along the *b* crystallographic axis (left) together with a schematic description of the packing (right).

It can be inferred that the formation of the "zwitterionic" complex from the reaction mixture under neutral conditions undergoes competitive prototropic equilibria between the different forms of the quinolinol which is strongly influenced by the presence of the metal ion. These equilibria involve both the quinolinolium (**H$_2$5,7ClQ$^+$**) and the quinolinolato (**5,7ClQ$^-$**) ions along with the zwitterionic form of the ligand, although the acidic character of the lanthanide ion may shift the equilibrium toward the protonated form. The tautomeric rearrangement of the neutral quinolinol in the complex is most likely due to the preference of the strong Lewis acid Yb^{3+} for anionic oxygen donor atoms. The coordination number of seven for Yb^{3+} in **YbClQ$_4$** is rather unusual because eight the most common for lanthanide complexes with organic ligands.[26] The stabilization of the monodentate zwitterionic coordinated quinolinols occurs through hydrogen bonding, and the steric hindrance provided by the chlorine atoms in the ligand periphery may prevent solvent molecules from entering the first coordination sphere.

Spectroscopic studies and photophysical properties

Lanthanide ion emission in complexes with "antenna" ligands usually occurs through a two-step mechanism, schematically depicted in Figure 3, that can be briefly summarized as follows. After optical excitation with visible or near-UV light, ligand singlet excited states S_1 can either decay to the ground state S_0, or to triplet states T_n through an intersystem crossing (ISC) mechanism. According to information available on 8-quinolinols and similar N-heterocycles, the energy of a triplet $^3(n–\pi^*)$ level (T_n) lies in between the lowest singlet $^1(\pi–\pi^*)$ (S_1) and the lowest triplet $^3(\pi–\pi^*)$ (T_1) states.[27–28] The upper energy levels of lanthanide ions can be subsequently populated through resonance energy transfer (RET) from ligand excited triplets that are close enough in energy.[29–34] Finally, the radiative decay $^{(2S+1)}\Gamma_{J'} \rightarrow {}^{(2S+1)}\Gamma_J$ yields emission of Ln^{3+}.[35–38] The Yb^{3+} complexes are often considered a "special case" among the class of emitting lanthanide complexes with respect to the sensitization process with antenna ligands; this is because there is only one receiving level, $^2F_{5/2}$, that can be populated by RET from an excited ligand. For efficient ligand-to-metal energy transfer, according to the Dexter mechanism ($\Delta J = \pm 1$),[39] the spectroscopic overlap between the emission band of the donor (the ligand) and the absorption band of the acceptor (the metal) should be effective. This outcome implies that the ligand donor (triplet) level should be low enough in energy to match well the ytterbium $^2F_{5/2}$ level ($\approx$10,000 cm^{-1}). For this reason several mechanisms such as photosensitization through internal redox processes[40,41] or phonon-assisted energy transfer from ligand triplet states[42] have been often invoked to account for ytterbium sensitization.

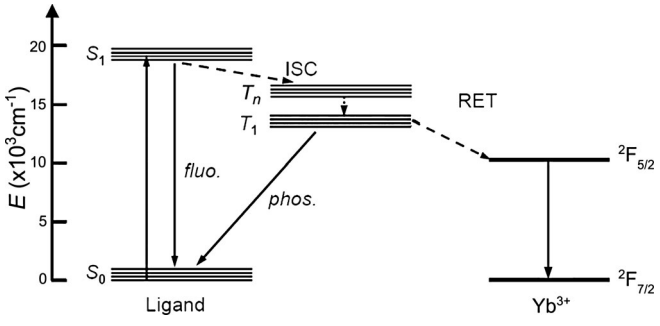

Figure 3. Jablonski diagram illustrating the energy levels of the quinolinolato ligand and the ytterbium ion and the photophysical processes leading to Yb^{3+} emission following ligand photoexcitation. Radiative decay of singlet or triplet excitons yields fluorescence (*fluo.*) or phosphorescence (*phos.*), respectively. Ytterbium radiative decay to the ground $^2F_{7/2}$ state yields emission at 1 μm. Dashed arrows represent nonradiative relaxation mechanisms.

To evaluate the overall (or absolute) luminescence quantum yield (Φ_{tot}) of sensitized luminescence from a lanthanide complex, Equation (1) can be applied:

$$\Phi_{tot} = \eta_{sens}\Phi_{Ln} = \eta_{sens}\tau_{obs}/\tau_{rad} \quad (1)$$

In this equation η_{sens} is the sensitization efficiency parameter representing the efficacy of ligand-to-metal energy transfer process and Φ_{Ln} is the intrinsic quantum yield for direct excitation of the lanthanide ion. The Φ_{Ln} value depends on the ratio between the rate constants of radiative ($\kappa_{rad} = 1/\tau_{rad}$) and excited-state deactivation ($\kappa_{obs} = 1/\tau_{obs}$) processes. The τ_{obs} value is the observed NIR decay time of a lanthanide compound and τ_{rad} is the "natural" radiative lifetime of a given lanthanide ion in a specific environment in the absence of nonradiative deactivation.[43–47]

Upon ligand photoexcitation in the near-UV, **YbClQ$_4$** shows dual luminescence in the visible (ligand-centered emission) and in the near infrared (metal-centered emission) regions, as reported below.

Ligand-centered optical properties

Electronic absorption of a solution of **YbClQ$_4$** in DMSO and solid-state diffuse reflectance (DR) spectra in the near UV-visible region of **YbClQ$_4$** are displayed in Figure 4. In the solution absorption spectrum two main ligand bands appear in the 300–500 nm region. Both the deprotonated and the zwitterionic forms of the quinolinolato ligand give a contribution to the more intense band falling near 340 nm. The band falling at about 394 nm is attributable to a $^1(\pi–\pi)^*$ ligand-centered transition with intraligand charge transfer (ILCT) character and closely reflects that of the deprotonated form of the ligand—

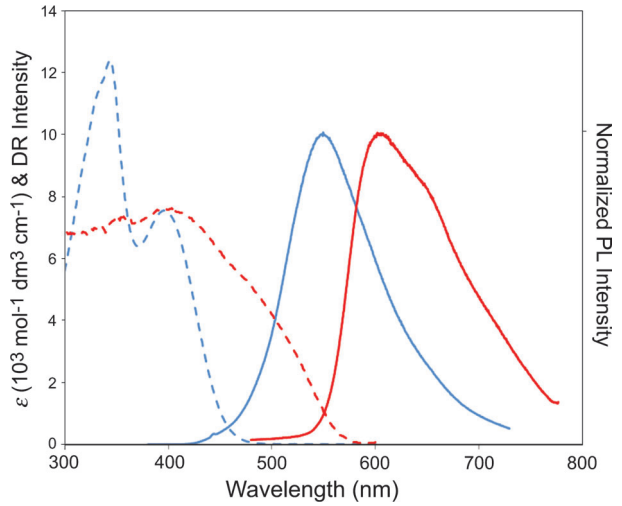

Figure 4. UV/Visible (electronic) absorption spectrum of **YbClQ$_4$** in DMSO solution (dashed blue line), solid state diffuse reflectance (DR; dashed red line, KBr pellet), and normalized photoluminescence (PL) spectra acquired after photoexcitation at 392 nm reported as solid lines (DMSO solution = blue line, crystalline sample = red line).

as can be expected for closed-shell metal complexes.[26] In the diffuse reflectance spectrum of a crystalline sample, the lowest absorption band becomes broader, undergoes a red-shift with respect to solution absorption, and displays a low-energy shoulder. After spectroscopic deconvolution[48] an additional maximum at 494 nm can be identified (see Figure S2 in the Supporting Information). This absorption accounts for the bright red color of the crystals compared to the yellow color of the complex in solution and can be assigned to a π–π^* intermolecular transition resulting from π stacking, which is particularly effective in this complex. This observation is in accordance with Brinkmann et al.,[49] who correlated the spectroscopic features of different crystalline phases of the tris-(8-quinolinolato)aluminum(III) (AlQ_3) to the density of the packing related to π–π orbital overlap between adjacent quinoline moieties.

Photoexcitation experiments on a solution of **YbClQ$_4$** in DMSO and crystals of **YbClQ$_4$** give the luminescence spectra which are reported in Figure 4. In solution, ligand fluorescence ($S_1 \rightarrow S_0$) centered at 545 nm is observed and is independent of the excitation wavelength in the whole ligand absorption region (see Figure S1). The corresponding fluorescence spectrum of the crystalline sample exhibits a remarkable red-shift with respect to solution luminescence of approximately 60 nm ($\lambda_{max} = 603$ nm). This "red" luminescence is related to the extensive π stacking of the aromatic ligands in the crystal arrangement and may be termed "excimer-like".[50] Meanwhile, no phosphorescence is observed at room temperature.

Near-infrared metal-centered optical properties

Photoexcitation of the quinolinolato ligand in the $^1(\pi$–$\pi)^*$ ligand band yields Yb^{3+} emission at about 1 μm. Near-infrared diffuse reflectance and photoluminescence spectra of crystals of **YbClQ$_4$** are reported in Figure 5.

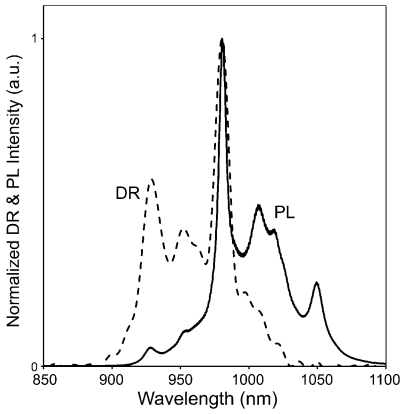

Figure 5. Normalized diffuse reflectance (DR; dashed line) and photoluminescence (PL; continuous line) spectra of crystals of **YbClQ$_4$** in the NIR region.

The Yb^{3+} $^2F_{5/2} \leftrightarrow {}^2F_{7/2}$ absorption and emission bands are moderately broadened and partially resolved into multiplets (Stark lines) owing to the partial removal of the degeneracy of 4f ground ($^2F_{7/2}$) and excited ($^2F_{5/2}$) levels into 2 J + 1 terms by crystal field effects, which makes f–f transitions partially allowed. The $^2F_{5/2}(0') \leftrightarrow {}^2F_{7/2}(0)$ transition peaks at about 977 nm in both photoluminescence and DR spectra. Lines at higher wavelengths are more intense and those at lower wavelengths in the photoluminescence (PL) spectrum are weaker than those found in the DR spectrum. This outcome is in agreement with the thermal population of the Stark sublevels of lanthanide ions. The observed fine structure arising from this Stark splitting is in accordance with the low symmetry of the metal environment.[35,41,47,51]

The photoluminescence decays under femtosecond laser pulse excitation were measured with an ultrafast photodiode. Monoexponential decays are observed in the near infrared region for both solid-state and anhydrous DMSO solutions, thus yielding similar ytterbium emission lifetimes of $\tau_{obs} = 7.10$ μs and $\tau_{obs} = 7.85$ μs, respectively (Figure 6). These values are comparable to those reported for analogous anhydrous ytterbium complexes with ligands derived from 8-hydroxy quinoline.[15,41,52–55]

To evaluate the intrinsic quantum yield, Φ_{Yb}, of ytterbium, the ytterbium "natural" radiative lifetime, τ_{rad}, has been experi-

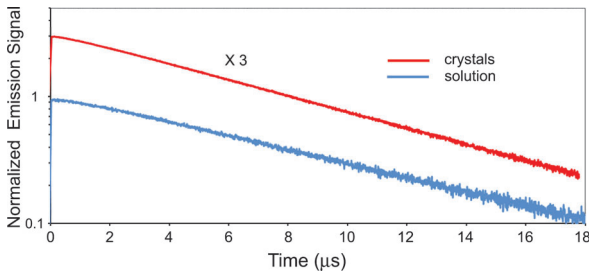

Figure 6. Normalized NIR experimental decay curves of **YbClQ$_4$** as crystalline sample (red line) and in DMSO solution (blue line). Emission signal is reported on a logarithmic scale.

mentally determined from spectroscopic data (absorption cross-section, σ_{Yb}) through the Strickler–Berg Equation (2):[56]

$$\kappa_{rad} = \tau_{rad}^{-1} = 8\pi n^2 c \frac{1}{\langle\lambda^3\rangle} \frac{2J+1}{2J'+1} \int \frac{\sigma_{Yb}(\lambda)}{\lambda} d\lambda \quad (2)$$

where n is the refractive index of the medium (1.48 for DMSO), c is the speed of light in vacuum and J and J′ refer to the ground and excited state, respectively. The ytterbium absorption cross-section in DMSO solution at 977 nm has been determined to be $\sigma_{Yb} = 1.9\text{x}10^{-20}$ cm^2.

The obtained value of $\tau_{rad} = 690$ μs perfectly matches the estimates for heterobinuclear Yb–Na chelates with benzoxazole-substituted 8-hydroxy quinolines,[51] thus demonstrating that in quinolinolate complexes the ytterbium ion shows remarkably high radiative strength. It must be underlined that these characteristic times are much shorter than the 1.2 or 2 ms values that have been previously reported and widely accepted.[57] Moreover, it is worth mentioning that much attention has to be paid in assessing radiative lifetimes in luminescent lanthanide complexes because significant underestimations of emission quantum yields may arise from their incorrect evaluation.

The decay time observed for ytterbium is about two orders of magnitude shorter with respect to the radiative lifetime, a fact that can be rationalized on the basis of to the so-called energy-gap law. It is in fact well known that the efficiency of lanthanide ions' NIR luminescence suffers severely from quenching phenomena mainly as a result of Förster resonance energy transfer (FRET)[58] from the emitting lanthanide ion to the strongly resonant oscillating CH groups present in the surroundings (deactivation through vibrational excitation). The solid-state diffuse reflectance (DR) spectrum, reported in Figure 7a (black curve), provides strong support for quenching through vibrational processes as a reasonable interpretation. In this spectrum two sharp peaks at 1670 and 1134 nm are observed which are related, respectively, to the second and third harmonic of the stretching vibration of aromatic CH groups of the ligand. As it can be seen from Figure 7a,b, where the energies of the superior harmonics of the CH stretching vibration are compared with those of the emitting levels of Yb^{3+} and Er^{3+} in the isostructural erbium complex $[Er(5,7ClQ)_2(H5,7ClQ)_2Cl]$ ($ErClQ_4$) as reference,[21] the ytterbium $^2F_{5/2} \rightarrow {}^2F_{7/2}$ emission is rather close in energy to the second CH vibrational overtone whereas the first overtone can be considered nonresonant. As a result, the intrinsic quantum yield found for **$YbClQ_4$** ($\Phi_{Yb} = 1.2\text{x}10^{-2}$) is about two orders of magnitude higher than that determined for the analogous $ErClQ_4$ complex ($\Phi_{Er} = 4.8\text{x}10^{-4}$) whose emission at 1.5 μm is instead extremely resonant with the ten-times more intense CH second vibrational harmonic (Figure 7a).[24] In fact, the vibrational transition probability considerably decreases with the vibrational quantum number, v, thus reducing quenching through vibrational excitation (energy-gap theory).[59]

To achieve a more quantitative understanding on the basis of structural and spectroscopic data in the framework of the Förster theory, the ytterbium (donor) emission quenching

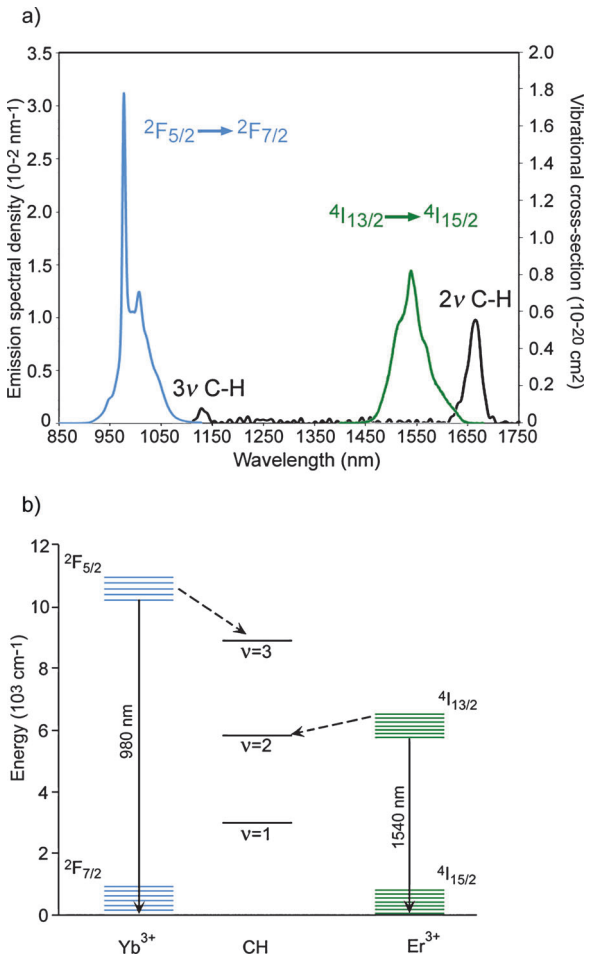

Figure 7. a) Diffuse reflectance spectrum (black curve extending from 1100 to 1750 nm and rescaled in terms of absorption cross-section per complex), of crystals of **$YbClQ_4$** dispersed on a Teflon film showing the 2nd (1670 nm) and 3rd (1134 nm) harmonics of stretching vibration of ligand CH groups and normalized NIR photoluminescence spectra of DMSO solutions of **$YbClQ_4$** (blue) and $ErClQ_4$ (green) acquired after photoexcitation at 392 nm. b) Energy gaps of emitting level manifolds of Yb^{3+} and Er^{3+} compared to the energy of the stretching mode of C–H groups and corresponding superior harmonics. Dashed arrows represent energy transfer to resonant harmonics of C–H stretching.

yield, Φ_{FRET}, resulting from energy transfer to the anharmonic CH oscillators (acceptors) has been evaluated by taking into account a power-law dependence on the dipole–dipole distance, r_j through Equations (3), (4), and (5):

$$\Phi_{FRET} = 1 - \frac{\kappa_{rad}}{\kappa_{FRET}} \quad (3)$$

$$\kappa_{FRET} = \kappa_{rad} \sum_j \left(\frac{R_{0,j}}{r_j}\right)^6 \quad (4)$$

$$R_{0,j}^6 = \frac{9\kappa_j^2}{128\pi^5 n^4} \int F_{Yb}(\lambda)\sigma_{CH}(\lambda)\lambda^4 d\lambda \quad (5)$$

where the j index refers to each CH acceptor and R_j represents the Förster distance, which is proportional to the overlap inte-

gral between the normalized Yb emission spectrum [$F_{Yb}(\lambda)$], and the vibrational absorption cross-section [$\sigma_{CH}(\lambda)$] of the acceptors. The κ^2 value is a geometrical factor that depends on the relative orientation between the transition dipoles of Yb^{3+} and the jth acceptor. The κ_{FRET} value is the donor–acceptor transfer rate. The resulting estimate for the quenching yield, Φ_{FRET}, is 0.45(5).

Similar results are obtained either with the discrete calculation or the continuous medium approximation using spectroscopic data of $ErClQ_4$ (Figure 7a) as the reference.[60] In the case of the anhydrous **$YbClQ_4$** complex, the role of water molecules in luminescence deactivation can be definitely ruled out. Nevertheless, a further small contribution to vibrational quenching may arise from the two N^+–H groups sharing hydrogen bonding with phenoxide units of the two deprotonated ligands as indicated by structural data (see Figure 1 and related description). However, no clear spectroscopic evidence can be found in the diffuse reflectance, although a series of very weak bands in the range 3200–2700 cm^{-1} in the FTIR spectrum (see Figure S3) might be related to these N^+–H groups. Unfortunately, lack of spectroscopic data hampers modeling of potential additional quenching effects that are clearly more relevant in **$YbClQ_4$** than in the corresponding isostructural erbium complex, $ErClQ_4$, where the overlap integral between the erbium emission band and the CH second overtone is much higher and the model accounts for over 99% of quenching effects.[23] It must also be mentioned that the similarity of solution and solid-state NIR decay times seems to rule out any additional external (matrix-related) deactivation channel.

Ligand-to-metal energy transfer

The overall luminescence quantum yield, Φ_{tot}, of **$YbClQ_4$** in DMSO solution has been measured, by using a solution of the corresponding erbium complex $ErClQ_4$ ($\Phi_{tot} = 3.8 \cdot 10^{-4}$) in the same solvent as reference, to yield a value of $1.4 \cdot 10^{-2}$.[24] The sensitization efficiency η_{sens}, calculated by Equation (1) from experimentally determined (observed) and radiative lifetimes (τ_{obs} and τ_{rad}) and quantum yield gives a value close to unity, thus demonstrating that very efficient energy transfer takes place from the quinolinolato ligand to the NIR-emitting ytterbium ion.

To better clarify this mechanism, combined transient PL and photoinduced absorption experiments with subpicosecond photoexcitation in the fundamental absorption band of the ligand, were performed and are summarized in Figure 8. Transient PL data, that are integrated over the excited singlet fluorescence emission spectrum (470–570 nm spectroscopic window), show that the singlet excited-state decay is prompt and occurs on an ultrafast timescale with time constants of the order of tens of ps for both solution and solid state samples, thus giving values that are in agreement with values found for analogous erbium quinolinolates.[11]

As shown in Figure 8a, the PL decay trace for crystals is resolution limited, and yields an excited singlet lifetime < 30 ps. In DMSO solution, the decay is biexponential with $\tau_1 = 53(1)$ and

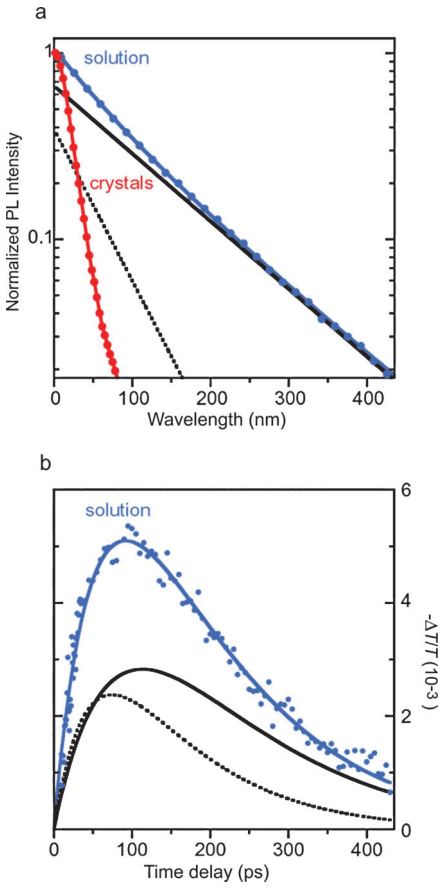

Figure 8. a) Transient photoluminescence of **$YbClQ_4$** as a crystalline sample (red dotted line) and in DMSO solution (blue dots). The signal is reported on a logarithmic scale. The blue line is the best fit based on a biexponential decay curve. Fit amplitude and decay time are $A_1 = 0.37(1)$ and $\tau_1 = 53(1)$ ps for the faster decay component (black dotted line), and $A_2 = 0.63(1)$ and $\tau_2 = 120(2)$ ps for the slower decay component (black solid line). b) Transient photoinduced absorption of **$YbClQ_4$**. Dots: Experimental data. Blue solid lines: best fit to experimental data. Black lines: Individual contributions of triplet excitons activated by the singlet exciton populations decaying as in the black lines in (a).

$\tau_2 = 120(2)$ ps time constants, possibly because of the coexistence of two populations of complexes with slightly different excited singlet kinetics. The characteristic times are much shorter than the value observed (8.5 ns) for AlQ_3, where the heavy-atom effect is negligible, thus suggesting that ligand singlet states in NIR-emitting lanthanide quinolinolates are strongly deactivated by intersystem crossing to ligand excited triplet states.[11] However, the observed intersystem crossing (ISC) is much faster than expected on the basis of the bare heavy-atom effect, for which the ISC time constant should scale with $1/Z^2$ (Z = atomic number of the metal ion) to yield values of the order of a few ns.[61]

Triplet dynamics has then been determined from the transient absorption signal probed by differential transmission ($\Delta T/T$) in DMSO solution in the 600–620 nm region where no singlet signal is detected (Figure 8b). Triplet population shows an ultrafast activation complementary to the excited singlet decay, followed by ultrafast decay, which is in agreement with previous reports for erbium quinolinolate complexes.[11] Quanti-

tative information can be extracted by fitting the measured excited triplet kinetics with the solution of a rate equation model for the excited singlet population, upon imposing the condition that the triplet activation time is equal to the singlet decay time. (Details of kinetic equations and curve fitting procedure are reported in the Supporting Information.) Curve fitting yields a triplet lifetime of approximately 110 ps. As lanthanide sensitization is virtually 100% efficient, the triplet lifetime is understood as being the time constant of the ligand-to-metal energy transfer process.

Triplet decay time for **$YbClQ_4$** is as fast as in erbium quinolinolates (80–100 ps) and much faster than that of gadolinium analogue ($\approx$1.4 ns), where no ligand-to-metal energy transfer can occur owing to the high energy of the Gd^{3+} first excited state.[62] This fast decay time clearly suggests that resonant energy transfer to upper energy levels of the metal is the main ligand triplet deactivation path and that external competitive ligand relaxation mechanisms such as triplet oxygen quenching,[63,64] or internal ILCT[65] do not affect the sensitization process and the overall luminescence quantum yield of NIR-emitting lanthanide quinolinolates.

It must be underlined that in quinolinolate complexes the triplet emission spectrum, as estimated from experiments done in AlQ_3,[27,66] is very broad, easily covering the 550–800 nm (18000–12500 cm^{-1}) range, hence so rendering energy transfer rather insensitive to lanthanide level alignment and absorption lineshape. Moreover, erbium is presumably sensitized in the $^4I_{11/2}$ level,[21] which is nearly resonant to the $^4F_{5/2}$ level of ytterbium. On the other hand, differences in sensitization times of ytterbium and erbium in quinolinolate complexes could be expected in view of the following facts: 1) The $^2F_{5/2} \leftarrow {}^2F_{7/2}$ absorption cross-section of ytterbium ($\approx 1.8\times10^{-20}$ cm^2) is about three times larger than the $^4F_{11/2} \leftarrow {}^4I_{15/2}$ absorption cross-section of erbium ($\approx 6\times10^{-21}$ cm^2; see Figure S4), and 2) Dexter-type transfer should be involved in the Yb sensitization (total angular momentum variation undergone by the lanthanide in the transfer process: $\Delta J = -1$) whereas Förster-type transfer should occur in the case of Er ($\Delta J = -2$). All the above-mentioned considerations should stimulate further theoretical efforts aimed at gaining more insight into the lanthanide energy-sensitization process and its dependence on ligand/lanthanide photophysical parameters. Photophysical properties of **$YbClQ_4$** in DMSO solution and as crystalline sample are summarized in Table 4.

Table 4. Photophysical parameters of **$YbClQ_4$** in anhydrous DMSO solution and in the solid state (crystal).

Sample	τ_{obs} [μs]	τ_{rad} [μs]	Φ_{tot} [%]	η_{sens} [%]
DMSO solution	7.85 (10)	690 (35)	1.40 (30)	95 (5)
solid state	7.10 (10)	–	–	–

Conclusion

Combined chemical and photophysical studies on the fully characterized novel anhydrous hepta-coordinated [Yb(5,7ClQ)$_2$(H5,7ClQ)$_2$Cl] complex that shows dual-luminescence in the visible and NIR regions, have allowed us to quantitatively characterize the photocycle and evaluate the most important factors that influence the emission process.

The ligand-to-metal sensitization efficiency has been determined to be close to unity, thus demonstrating that quinolinolato ligands are extremely efficient antennas toward NIR-emitting lanthanide ions. Combined transient photoluminescence and photoinduced absorption experiments show that ligand-to-metal energy transfer involves the triplet states of the ligand and that ISC occurs on an ultrafast timescale with time constants much shorter than values expected on the basis of the bare heavy-atom effect. Resonant energy transfer from ligand triplet states to the metal takes place with a time constant comparable to values found in erbium quinolinolate complexes.

The remarkably high radiative strength of Yb^{3+} found in [Yb(5,7ClQ)$_2$(H5,7ClQ)$_2$Cl] is in contrast to values of the ytterbium radiative lifetime often taken into account in the literature. However, observed NIR lifetimes are two orders of magnitude shorter than radiative lifetime because of quenching effects ascribed to vibrational deactivation through CH groups of the ligand. These nonradiative decay processes have been quantitatively assessed on the basis of structural and spectroscopic data by taking into account the transfer rate of excitation from the emitting Yb ion to the accepting CH oscillators, according to the Förster theory. The model accounts for approximately 50% of quenching effects, in contrast to the case of the corresponding Er complex, where 99% quenching was achieved. Thus hinting at additional nonradiative paths for which no clear experimental evidence has been found so far.

Experimental Section

General

All the reagents and solvents were purchased from Aldrich and used without further purification. The synthesis was carried out following a procedure which has shown to work well to obtain analogous Er, Gd complexes with H5,7ClQ.[20,21] Electronic UV/Vis-NIR: Diffuse reflectance (DR) on KBr pellets and Teflon films and absorption spectra were collected using a Varian Cary 5 spectrophotometer. Vibrational FTIR spectra on KBr pellets were collected using a Bruker Equinox 55 spectrophotometer. FT-Raman spectra of crystalline samples were collected using a Bruker RFS/100S spectrometer operating in a back-scattering geometry with a Nd:YAG (1064 nm) laser source. Elemental analysis data were collected using a Carlo Erba mod. EA1108 CHNS analyzer.

Synthesis of [Yb(5,7ClQ)$_2$(H5,7ClQ)$_2$Cl] ($YbClQ_4$)

A solution of $YbCl_3{\cdot}6H_2O$ in CH_3CN/CH_3OH (4:1 v/v; 10 mL) was slowly added to a solution of 5,7-dichloro-8-quinolinol (1:4 ratio) dissolved in the same solvent mixture at 50–60 °C. After 24 h the yellow mixture was dried under vacuum until it turned orange and was left standing to the air. Any ligand excess that may precipitate after crystallization of the complex was removed by washing with diethyl ether. After three days red crystals, suitable for X-ray studies, were collected and washed with diethyl ether (yield 53%). Ele-

mental analysis calcd for $C_{36}H_{18}L_9YbN_4O_4$: C 40.95 (40.69), H 1.63 (1.71), N 5.43 (5.27); FT-IR (KBr pellet, cm^{-1}): 3236 vw, 3171 vw, 3102 w, 3026 w, 2966 w, 2914 w, 2850 vw, 2752 vw, 2116 w (ν, N^+–H), 2013 w, 1616 m, 1592 w, 1560 s, 1544 m, 1489 m, 1455 vs, 1394 m, 1364 s, 1314 m, 1292 w, 1250 w, 1232 mw, 1220 m, 1194 m, 1144 m, 1106 m (split peak), 1051 mw (δ, C–H), 991 vw, 957 m (ν, C–Cl), 876 m (ν, C–Cl), 810 m, 789 m, 749 s (split peak), 672 m, 659 m, 646 w, 634 m, 585 w, 571 mw, 505 m, 422 mw; FT-Raman (cm^{-1}): 3106 m, 3068 s, 2887 m, 1591 s, 1572 s, 1561 m, 1470 m, 1360 vs, 1294 mw, 1145 m, 1051 m (δ, C–H), 799 m, 763 m, 668 m, 570 m, 504 m, 407 w; electronic absorption spectroscopy, DMSO (nm; [mol^{-1} dm^3cm^{-1}]): 343[$(12.41\pm0.03)10^3$], 396[$(7.55\pm0.02)10^3$]; diffuse reflectance (Teflon film, nm): 268, 351 sh, 405, 480 sh; 928, 952, 979 (split, $^2F_{7/2}\rightarrow{}^2F_{5/2}$); 1134 (3 ν, C–H); 1667 (2 ν, C–H).

Data collection and structure determination

Single-crystal data were collected using a Bruker AXS Smart 1000 area detector diffractometer ($Mo_{K\alpha}$; $\lambda = 0.71073$ Å). Cell constants were obtained from a least-square refinement of selected strong reflections distributed over a hemisphere of the reciprocal space.[67] No crystal decay was observed. Absorption correction using the program SADABS[68] was applied and resulted in minimum and maximum transmission factors of 0.907–1.000. The structure was solved by direct methods (SIR97)[69] and refined with full-matrix least squares (SHELXL-97),[70] using the Wingx software package.[71] Nonhydrogen atoms were refined anisotropically. The hydrogen atoms of the protonated quinoline molecules were ligated to the nitrogen atoms in agreement with the molecular structures of the isostructural Er and Gd complexes.[21, 22] The hydrogen atoms were placed at their calculated positions. The maximum and minimum peaks on the final difference Fourier maps corresponded to 0.925 and -0.566 e Å^{-3}. Graphical material was prepared with the and Mercury 2.0 program.[72]

Transient optical spectroscopy

Photoluminescence (PL) and photoinduced absorption are excited at 392 nm wavelength by the frequency-doubled output pulses of a regenerative Ti:Sapphire amplifier (Quantronix INTEGRA C) running at repetition frequency of 1 kHz. The PL transient is spectroscopically dispersed in a 0.3 m imaging spectrograph (Acton SpectraPro 2300i) and captured by a streak camera (Hamamatsu C5680) operating in single-shot mode. Experimental data show that effective temporal resolution is better than 30 ps under the operating conditions (with 70–100 s accumulation time). Photoinduced absorption is probed by broadband synchronous pulses obtained by supercontinuum generation in a sapphire plate. The optical probe beam transmitted through the sample is spectroscopically dispersed using a SpectraPro 2300i spectrograph and detected by a charge-coupled device (Andor NEWTON). Pump-probe time delay is varied using a motorized optical delay stage. Photoinduced absorption is measured as the differential transmission signal $\Delta T/T = (T\text{-}T_0)/T_0$, where T (T_0) is the transmitted probe pulse energy in presence (absence) of the pump pulse. Near-infrared emission transients are measured using a DC-125 MHz NIR photoreceiver (NewFocus 1811) and a 1 GHz digitizing oscilloscope (Tektronik TDS 5104). Photoexcitation fluences were kept below the level of one excitation per complex per laser pulse in all experiments.

Acknowledgements

The Regione Autonoma della Sardegna is gratefully acknowledged for financial support through POR Sardegna FSE 2007–2013, L.R.7/2007 "Promozione della ricerca scientifica e dell'innovazione tecnologica in Sardegna". (Research Project: "Complessi di lantanidi con proprietà di luminescenza nel vicino infrarosso: studio della correlazione struttura/proprietà fotofisiche indirizzato alla fotonica molecolare" (CRP-17571) and the Cofinanced Research Grant of F.A.: "Complessi di lantanidi come materiali luminescenti per applicazioni in fotonica" (CRP2 502)). Mauro Aresti and Elisa Sessini are acknowledged for technical support.

Keywords: lanthanides · luminescence · stacking interactions · time-resolved spectroscopy · ytterbium

[1] R. J. Curry, W. P. Gillin, *Appl. Phys. Lett.* **1999**, *75*, 1380.
[2] W. P. Gillin, R. J. Curry, *Appl. Phys. Lett.* **1999**, *74*, 798.
[3] O. M. Khreis, R. J. Curry, M. Somerton, W. P. Gillin, *J. Appl. Phys.* **2000**, *88*, 777.
[4] O. M. Khreis, W. P. Gillin, M. Somerton, R. J. Curry, *Org. Electron.* **2001**, *2*, 45.
[5] R. J. Curry, W. P. Gillin, *Synth. Met.* **2000**, *111–112*, 35.
[6] R. J. Curry, W. P. Gillin, A. P. Knights, R. Gwilliam, *Opt. Mater.* **2001**, *17*, 161.
[7] Z. R. Hong, C. J. Liang, R. G. Li, D. Zhao, D. Fan, W. L. Li, *Thin Solid Films* **2001**, *391*, 122.
[8] Z.-F. Chen, X.-Y. Song, Y. Peng, X. Hong, Y.-C. Liu, H. Liang, *Dalton Trans.* **2011**, *40*, 1684.
[9] Y. Kawamura, Y. Wada, M. Iwamuro, T. Kitamura, S. Yanagida, *Chem. Lett.* **2000**, 280.
[10] F. Artizzu, M. L. Mercuri, A. Serpe, P. Deplano, *Coord. Chem. Rev.* **2011**, *255*, 2514, and references therein.
[11] F. Quochi, M. Saba, F. Artizzu, M. L. Mercuri, P. Deplano, A. Mura, G. Bongiovanni, *J. Phys. Chem. Lett.* **2010**, *1*, 2733.
[12] a) M. Iwamuro, T. Adachi, Y. Wada, T. Kitamura, S. Yanagida, *Chem. Lett.* **1999**, 539; b) M. Iwamuro, T. Adachi, Y. Wada, T. Kitamura, N. Nakashima, S. Yanagida, *Bull. Chem. Soc. Jpn.* **2000**, *73*, 1359.
[13] a) J. Thompson, R. I. R. Blyth, G. Gigli, R. Cingolani, *Adv. Funct. Mater.* **2004**, *14*, 979; b) R. I. R. Blyth, J. Thompson, Y. Zou, R. Fink, E. Umbach, G. Gigli, R. Cingolani, *Synth. Met.* **2003**, *139*, 207.
[14] A. Nonat, D. Imbert, J. Pécaut, M. Giraud, M. Mazzanti, *Inorg. Chem.* **2009**, *48*, 4207.
[15] N. M. Shavaleev, R. Scopelliti, F. Gumy, J.-C. G. Bünzli, *Inorg. Chem.* **2009**, *48*, 2908.
[16] G. F. de Sà, O. L. Malta, C. de Mello Donegá, A. M. Simas, R. L. Longo, P. A. Santa- Cruz, E. F. da Silva, *Coord. Chem. Rev.* **2000**, 196, 165.
[17] N. Sabbatini, M. Guardigli, J.-M. Lehn, *Coord. Chem. Rev.* **1993**, 123, 201.
[18] J. M. Lehn, *Angew. Chem.* **1990**, *102*, 1347; *Angew. Chem. Int. Ed. Engl.* **1990**, *29*, 1304.
[19] a) R. Van Deun, P. Fias, P. Nockemann, A. Schepers, T. N. Parac-Vogt, K. Van Hecke, L. Van Meervelt, K. Binnemans, *Inorg. Chem.* **2004**, *43*, 8461; b) R. Van Deun, P. Fias, P. Nockemann, K. Van Hecke, L. Van Meervelt, K. Binnemans, *Eur. J. Inorg. Chem.* **2007**, 302; c) R. Van Deun, P. Fias, K. Driesen, K. Binnemans, C. Görller-Walrand, *Phys. Chem. Chem. Phys.* **2003**, *5*, 2754.
[20] F. Artizzu, P. Deplano, L. Marchiò, M. L. Mercuri, L. Pilia, A. Serpe, F. Quochi, R. Orrù, F. Cordella, F. Meinardi, R. Tubino, A. Mura, G. Bongiovanni, *Inorg. Chem.* **2005**, *44*, 840.
[21] F. Artizzu, P. Deplano, L. Marchiò, M. L. Mercuri, L. Pilia, A. Serpe, F. Quochi, R. Orrù, F. Cordella, M. Saba, A. Mura, G. Bongiovanni, *Adv. Funct. Mater.* **2007**, *17*, 2365.
[22] F. Artizzu, K. Bernot, A. Caneschi, E. Coronado, J. M. Clemente-Juan, L. Marchiò, M. L. Mercuri, L. Pilia, A. Serpe, P. Deplano, *Eur. J. Inorg. Chem.* **2008**, 3820.

[23] F. Quochi, R. Orrù, F. Cordella, A. Mura, G. Bongiovanni, F. Artizzu, P. Deplano, M. L. Mercuri, L. Pilia, A. Serpe, *J. Appl. Phys.* **2006**, *99*, 053520.
[24] F. Quochi, F. Artizzu, M. Saba, F. Cordella, M. L. Mercuri, P. Deplano, M. A. Loi, A. Mura, G. Bongiovanni, *J. Phys. Chem. Lett.* **2010**, *1*, 141.
[25] a) H. Gershon, M. W. McNeil, S. G. Shulman, J. W. Parkes, *Anal. Chim. Acta* **1972**, *62*, 43; b) F. Goldman, E. L. Wehry, *Anal. Chem.* **1970**, *42*, 1178.
[26] C. Huang in *Rare Earth Coordination Chemistry, Fundamentals and Applications*, Wiley-VCH, Weinheim, **2010**.
[27] R. Ballardini, G. Varani, M. T. Indelli, F. Scandola, *Inorg. Chem.* **1986**, *25*, 3858.
[28] K. Lower, M. A. El-Sayed, *Chem. Rev.* **1966**, *66*, 199.
[29] J. Kido, Y. Okamoto, *Chem. Rev.* **2002**, *102*, 2357.
[30] B. W. Van der Meer, G. Coker, S. Y. S. Chen in *Resonance Energy Transfer Theory and Data*, Wiley, New York, **1994**.
[31] R. D. Archer, H. Y. Chen, L. C. Thompson, *Inorg. Chem.* **1998**, *37*, 2089.
[32] F. Gutierrez, C. Tedeschi, L. Maron, J. P. Daudey, R. Poteau, J. Azema, P. Tisnes, C. Picard, *Dalton Trans.* **2004**, 1334.
[33] S. Sato, M. Wada, *Bull. Chem. Soc. Jpn.* **1970**, *43*, 1955.
[34] M. Latva, H. Takalo, V. M. Mukkala, C. Matachescu, J. C. Rodriguez-Ubis, J. Kankare, *J. Lumin.* **1997**, *75*, 149.
[35] H. Wang, G. Qian, M. Wang, J. Zhang, Y. Luo, *J. Phys. Chem. B* **2004**, *108*, 8084, and references therein.
[36] P. A. Tanner, C.-K. Duan, *Coord. Chem. Rev.* **2010**, *254*, 3026, and references therein.
[37] S. V. Eliseeva, J.-C. G. Bünzli, *Chem. Soc. Rev.* **2010**, *39*, 189.
[38] a) B. R. Judd, *Phys. Rev.* **1962**, *127*, 750; b) G. S. Ofelt, *J. Chem. Phys.* **1962**, *37*, 511.
[39] D. L. Dexter, *J. Chem. Phys.* **1953**, *21*, 836.
[40] W. D., Jr. Horrocks, J. P. Bolender, W. D. Smith, R. M. Supkowski, *J. Am. Chem. Soc.* **1997**, *119*, 5972.
[41] Y. Zhong, L. Si, H. He, A. G. Sykes, *Dalton Trans.* **2011**, *40*, 11389.
[42] C. Reinhard, H. U. Güdel, *Inorg. Chem.* **2002**, *41*, 1048.
[43] J.-C. G. Bünzli, C. Piguet, *Chem. Soc. Rev.* **2005**, *34*, 1048.
[44] J.-C. G. Bünzli, C. Piguet, *Chem. Rev.* **2002**, *102*, 1897.
[45] J.-C. G. Bünzli, A.-S. Chauvin, H. K. Kim, E. Deiters, S. V. Eliseeva, *Coord. Chem. Rev.* **2010**, *254*, 2623.
[46] M. H. V. Werts, J. W. Verhoeven, J. W. Hofstraat, *J. Chem. Soc. Perkin Trans.* **2000**, *2*, 433.
[47] R. F. Ziessel, G. Ulrich, L. Charbonnière, D. Imbert, R. Scopelliti, J.-C. G. Bünzli, *Chem. Eur. J.* **2006**, *12*, 5060.
[48] PeakFit v. 4.12 program, Systat Software.
[49] a) M. Brinkmann, G. Gadret, M. Muccini, C. Taliani, N. Masciocchi, A. Sironi, *J. Am. Chem. Soc.* **2000**, *122*, 5147; b) H. Kaji, Y. Kusaka, G. Onoyama, F. Horii, *J. Am. Chem. Soc.* **2006**, *128*, 4292.
[50] a) N. K. Al-Rasbi, C. Sabatini, F. Barigelletti, M. D. Ward, *Dalton Trans.* **2006**, 4769; b) X. Mou, Y. Wu, S. Liu, M. Shi, X. Liu, C. Wang, S. Sun, Q. Zhao, X. Zhou, W. Huang, *J. Mater. Chem.* **2011**, *21*, 13951.
[51] E. G. Moore, J. Xu, S. C. Dodani, J. Jocher, A. D'Aléo, M. Seitz, K. N. Raymond, *Inorg. Chem.* **2010**, *49*, 4156.
[52] N. M. Shavaleev, R. Scopelliti, F. Gumy, J.-C. G. Bünzli, *Inorg. Chem.* **2009**, *48*, 7937.
[53] G. Bozoklu, C. Marchal, J. Pécaut, D. Imbert, M. Mazzanti, *Dalton Trans.* **2010**, *39*, 9112.
[54] M. Albrecht, O. Osetska, J. Klankermayer, R. Fröhlich, F. Gumy, J.-C. G. Bünzli, *Chem. Commun.* **2007**, 1834.
[55] A. Nonat, D. Imbert, J. Pécaut, M. Giraud, M. Mazzanti, *Inorg. Chem.* **2009**, *48*, 4207.
[56] S. J. Strickler, R. A. J. Berg, *Chem. Phys.* **1962**, *37*, 814.
[57] a) M. H. V. Werts, R. T. F. Jukes, J. W. Verhoeven, *Phys. Chem. Chem. Phys.* **2002**, *4*, 1542; b) S. I. Klink, L. Grave, D. N. Reinhoudt, F. C. J. M. Van Veggel, M. H. V. Werts, F. A. J. Geurts, J. W. Hofstraat, *J. Phys. Chem. A* **2000**, *104*, 5457.
[58] a) T. Főrster, *Discuss. Faraday Soc.* **1959**, *27*, 7; b) T. Förster, *Annalen der Physik* **1948**, *2*, 55, English Translation, **1993**.
[59] S. Yanagida, Y. Hasegawa, K. Murakoshi, Y. Wada, N. Nakashima, T. Yamanaka, *Coord. Chem. Rev.* **1998**, *171*, 461.
[60] In the continuous model approximation, the average acceptor density (ρ_{CH}) replaces the discrete quenchers distribution. R_{min}, that is, the minimum distance between the lanthanide ion and the acceptors, below which $\rho_{CH}=0$ is also taken into account, see reference [23]. For **$YbClQ_4$** the following values were obtained: $\sigma_{CH}\approx 6x10^{--22}$ cm^2, $\rho_{CH}=8.03x10^{21}$ cm^{-3}, $R_{min}=3.490$ Å. Vibrational absorption cross-section was evaluated from the diffuse reflectance spectrum of the isostructural Gd complex (see Ref. [22]) in which no lanthanide absorption near 1 μm is found. Baseline correction was applied to offset background noise as a result of light aberration in crystal samples. The CH absorption was fitted with a Voigt function.
[61] D. Beljonne, Z. Shuai, G. Pourtois, J. L. Brédas, *J. Phys. Chem. A* **2001**, *105*, 3899.
[62] A. Strasser, A. Vogler, *Inorg. Chim. Acta* **2004**, *357*, 2345.
[63] S. I. Klink, G. A. Hebbink, L. Grave, F. C. J. M. Van Veggel, D. N. Reinhoudt, L. H. Slooff, A. Polman, J. W. Hofstraat, *J. Appl. Phys.* **1999**, *86*, 1181.
[64] S. I. Klink, L. Grave, D. N. Reinhoudt, F. C. J. M. Van Veggel, M. H. V. Werts, F. A. J. Geurts, J. W. Hofstraat, *J. Phys. Chem. A* **2000**, *104*, 54571.
[65] M. Albrecht, O. Osetska, J. Klankermayer, R. Fröhlich, F. Gumy, J.-C. G. Bünzli, *Chem. Commun.* **2007**, 1834.
[66] H. D. Burrows, M. Fernandes, J. S. de Melo, A. P. Monkman, S. Navaratnam, *J. Am. Chem. Soc.* **2003**, *125*, 15310.
[67] SMART (control) and SAINT (integration)software for CCD systems, Bruker AXS, Madison, WI, USA, **1994**.
[68] *Area-Detector Absorption Correction*; Siemens Industrial Automation, Inc., Madison, WI, USA, **1996**.
[69] A. Altomare, M. C. Burla, M. Camalli, G. L. Cascarano, C. Giacovazzo, A. Guagliardi, A. G. G. Moliterni, G. Polidori, R. Spagna, *J. Appl. Crystallogr.* **1999**, *32*, 115.
[70] G. M. Sheldrick, *SHELX97: Programs for Crystal Structure Analysis* (release 97 – 2), **1997**, University of Göttingen, Germany.
[71] L. J. Farrugia, *J. Appl. Crystallogr.* **1999**, *32*, 837.
[72] C. F. Macrae, P. R. Edgington, P. McCabe, E. Pidcock, G. P. Shields, R. Taylor, M. Towler, J. van de Streek, *J. Appl. Crystallogr.* **2006**, *39*, 453.

Received: January 12, 2012
Published online on February 15, 2012

